

# A Ptolemaic approach improving the conjunction analysis pipeline for LEO

De Marchi Pietro<sup>a</sup>

<sup>a</sup>*AIKO srl, Via dei Mille 22, Turin, 10123, Italy,*

---

## Abstract

Low-Earth-Orbit (LEO) region congestion is becoming one of the big issues of the modern space era. To avoid the Kessler syndrome, now more than ever it is needed to improve awareness about space traffic, and upgrade the entire monitoring process. Extensive literature is available covering the topics of orbital conjunction filtering techniques and computation of the Minimum Orbital Intersection Distance (MOID). The present paper investigates an alternative filtering method exploiting the near-circularity of certain orbits (a condition often verified in LEO), to improve conjunction analysis performance. Elliptical orbits are reshaped through an auxiliary *deferent* model, inspired by C. Ptolemy's orbital theory, replacing the real motion along conjunction analysis. To recover satellites' averaged mean orbital elements, CelesTrack LEO catalogue was considered and propagated. Based on averaged parameters, off-centric circular orbits are considered instead of elliptical ones. The resulting deferents (off-centric circles) are not far from osculating orbits due to LEOs low eccentricities, becoming the basis for the conjunction analysis algorithm. The algorithm is conceived as a sequence of pre-filters and a final MOID computation. Performances are inspected through an all-vs-all analysis, taking as reference a combination of Hoots' and Gronchi's algorithms. This method achieves good performance as compared with these traditional benchmarks. Adopting this approach could reduce the time needed for a preliminary conjunction inspection during the first phases of the Collision Avoidance (CA) process, especially in LEO, where pre-filtering aims to reduce the number of orbit couples where precise MOID computation is needed.

*Keywords:* conjunction, MOID, orbit, propagation

---

## 1. Introduction

The LEO region overcrowding is a very well-known problem in the space sector, especially for all kinds of human activities in space. While the Kessler syndrome (from the hypothesis of Donald J. Kessler in 1978) is still preventable today, the number of new mega-constellations and small satellites grow consistently. Furthermore, this escalation is not properly regulated, causing often undesired collisions and consequently uncontrolled debris. As reported in the Space Sustainability bulletin [1] (issue of December 2022) of the French company *Share my Space* about space sustainability, just in the last month of 2022: more than 286 new debris was produced, and around six tons of objects orbiting Earth below the 1 000 km have been estimated. Between these, about 10 000 are satellites and around 1 000 are rocket bodies. This situation is well represented by the picture reported in the report itself, Figure 1.

Consequently, the plan and management of upcoming missions require more and more efficient and wise procedures for collision avoidance. All nations and space communities should share data and common means to face this space crisis. The main pragmatic issue is the amount of orbits pairs to check for future close encounters, due to the high volumes of objects resident in LEO. This implies that ground operators need a more automatized, efficient and at the same time precise framework for possible conjunctions identification.

This paper proposes an alternative approach for conjunction detection based on an orbit approximation valid especially in

LEO region (the most critical for traffic management). Routines capable of efficiently eliminating couples, or stating that two satellites will never come closer than a certain distance in time are usually called *filters* or *pre-filters*. Algorithms computing the MOID, are called by the acronym itself: the MOID is mathematically the absolute minimum of the Euclidean distance between orbits. One of the first approaches to the topic was by G. Sitarsky [2] in 1968, later expanded through the collaboration with Hoots et al. [3], presenting an analytical formulation for relative distances between elliptical orbits. After them, Kholoshenikov and Vassiliev [4], later Gronchi [5] in 2005 and Bonanno [6] work all on the polynomial roots for minimum distance computations. In particular, Gronchi developed one of the most efficient routines of this type, applying the fast Fourier transformation to the orbital MOID problem. In 2010 Armellini et al [7] propose instead a global optimization for the resolution of the MOID problem.

In recent times the same techniques have been applied also to asteroids, like the more recent works of Milani [8], Rozek in 2011 [9] and many others.

The present approach proposes a series of pre-filters and a final MOID focus on LEO objects, based on the assumption of replacing the classical Keplerian elliptical orbit formulation with its auxiliary circle or the so-called *deferent*. The *deferent* term is employed here since the inspiration for this idea

Owner	Current number of objects	Jan 1 <sup>st</sup> 2022
USA	9970	8548
CIS (Russia)	7588	9075
CHINA	5049	4466
FRANCE	581	580
UK	555	447
JAPAN	292	364
INDIA	217	218
GLOBALSTAR	156	164
ESA	144	147
INTELSAT	92	92
SES	86	81
CANADA	81	76
GERMANY	78	77
EUTELSAT	61	57

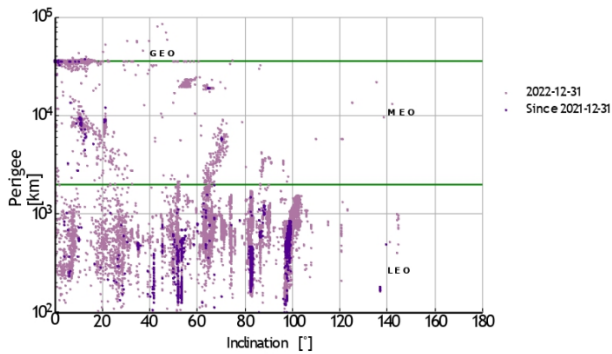


Figure 1: Summary of the main satellite owners (top) and the distribution by inclination and perigee of resident objects up to GEO (down). Credits: [1].

comes from the readings about the ancient C. Ptolemy’s<sup>1</sup> solar system model. This simplification consists in considering an off-centric circle instead of the ellipse (Keplerian model). This condition is especially suitable for LEO orbits, which are for the great majority almost circular. This peculiarity is also particularly promising for integration in an ML (Machine Learning) approach, this will be treated later once the outcomes of the present approach will be highlighted. In 2021 Stevenson E. et al. [10] presented a study about the improvements carried by an AI-based pre-filtering analysis in terms of computational time efficiency.

The present paper is organised as follows. Firstly, the physical background behind the algorithm itself is discussed. Later, performance is assessed through the comparison with Gronchi’s algorithm combined with Hoots’ prefilters [11]. The orbit dataset employed for the comparison is the entire LEO catalogue’s TLEs (Two Lines Elements, [12]) of satellites, retrieved from SpaceTrack [13] on January 10, 2023.

## 2. Hardware employed

All results involving performance evaluations of the algorithms developed for this research have been produced on the same hardware, here reported its main features for repeatability and comparison:

- CPU: 11th Gen Intel®Core™i5-1135G7 2.40GHz × 8
- OS: Ubuntu 22.04.1 LTS, 64-bit
- Code language: Python 3.8

## 3. Conjunction analysis process

### 3.1. Pipeline overview

This chapter provides a brief overview of a typical pipeline of space conjunction analysis to understand better at which stage the present research can contribute. First of all space objects are tracked through ground telescope networks, e.g. the United States Surveillance Space Network (SSN) is the main reference in monitoring space around Earth. Once TLEs are generated for untracked objects or updated for already known ones, TLEs are uploaded to the catalogue. Usually the United States Space Force, through NORAD, updates the SpaceTrack catalogue. TLE is the most employed format for cataloguing the space objects once detected, containing satellite NORAD identifier and orbital parameters data (orbital elements and drag data).

The orbit information contained in TLEs can be extracted properly only through the SGP4 propagator [14], allowing to recover the osculating contributions in time (the employment of SGP4 in this context is also treated later when the catalogue is employed effectively). After the propagation with SGP4, all the orbits are propagated through more accurate methods together with their covariance. The last step is the all-vs-all analysis aiming to find close encounters: all the orbits are inspected in couples looking for close encounters. Since the number of comparisons nowadays is huge (in order to compare 7 000 objects, one should evaluate 24 496 500 orbit couples) *pre-filters* are employed to quickly exclude couples that would certainly not experience a close encounter. The process of filtering and propagation can be inverted sometimes. In any case, this catalogue inspection happens at least six days ahead of the possible events. Ultimately, once close approach candidates are detected, a refinement of the estimate and accurate analysis is conducted about a small subset. If the conjunction is confirmed, a collision data message (CDM) is delivered to the operator with collision probability indications. For example, the United States Combined Space Operations Center (CSpOC) generally delivers messages around three days in advance of the event.

The method proposed in this paper could contribute to speeding up the filtering phase and in general the very first part of catalogue analysis. Since the object’s propagation is linked to the filtering phase the approximated orbital model is conceived also as built-up on the propagation information of the orbit. Another crucial point in the previous pipeline is the number of messages dispatched: a satellite operator receives approximately tens of thousands of CDMs per month. Relatively to this last turning point, the present algorithm could help in forecasting the orbit behaviour about close encounters. However, modern pipelines for collision avoidance in control centres are all based on classical approaches. AI-based approach could really improve the efficiency of such time-consuming

<sup>1</sup>Claudius Ptolemy (Latin: Claudius Ptolemaeus) (c.100 – c.170 AD) was a mathematician, astronomer, geographer, and astrologer; lived in Egypt at the times of the Roman empire.

### 3.2. The actual LEO environment

Before moving to the description of the Ptolemy approximation and the filter structure itself, a brief analysis of the LEO environment characteristics is presented. Figure 2 reports the orbital parameters distribution for the TLEs retrieved. The satellites considered for the present study are active and inactive ones orbiting in the LEO region (means mean motion higher than 11.25 and eccentricity less than 0.25) stored in the SpaceTrack catalogue through TLEs. The TLEs retrieved are 7757.

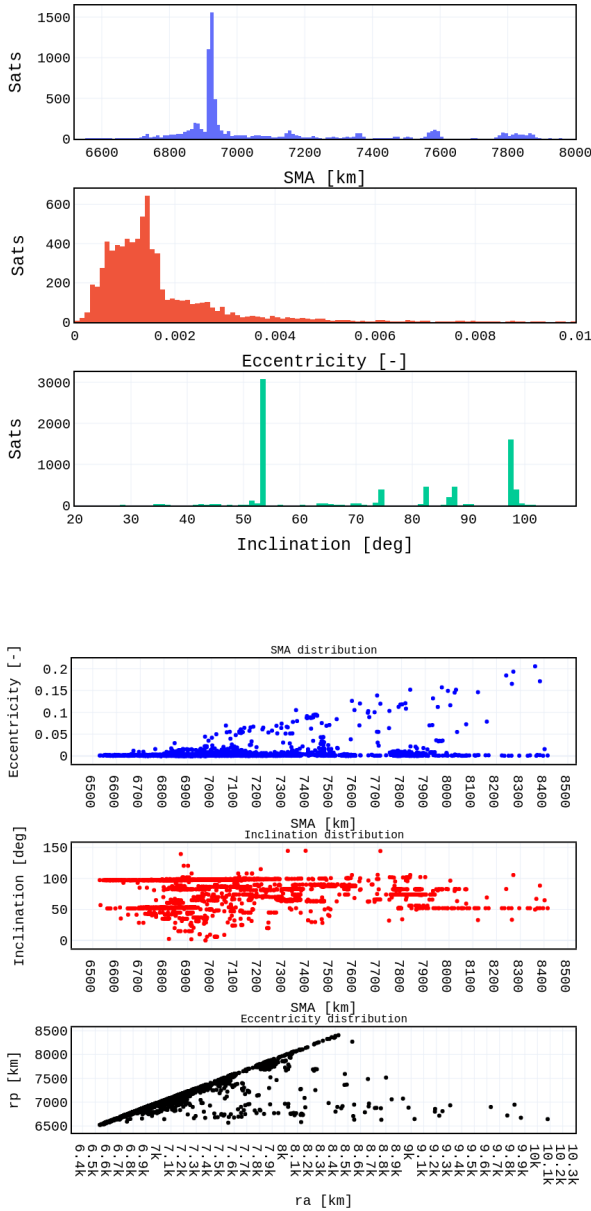


Figure 2: Visualization of TLEs' most relevant parameters distribution.

The Keplerian parameters plotted (semi-major-axis  $a$ , inclination  $i$  and eccentricity  $e$ ) are recovered from TLEs through an SGP4 forward propagating of 10 seconds. These are directly plotted just to give evidence of the distributions. These plots

show some interesting well known typical patterns in LEO. First of all LEO orbits gather around certain values of eccentricities and inclination: eccentricities values are very small and usually under 0.05, while for inclination there is a tendency for retrograde orbits or inclination around 50 deg (in general all between 50 and 100 deg). Furthermore, the clearest trend is in the ratio between  $ra$  (apogee radius) and  $rp$  (perigee radius), due to the decay limits of orbits in LEO. Coming back specifically to eccentricities, Table 1 reports statistics about eccentricity: these values show that objects in LEO can be assumed to follow almost circular orbits (presenting sufficiently small eccentricities).

Table 1: Eccentricities distribution in the catalogue (7757 satellites retrieved).

Range	N° satellites	Percentage of orbits
$e < 0.05$	7670	98%
$e < 0.01$	7523	96%
$e < 0.005$	7284	93%
$e < 0.001$	2275	29%

The last point is about perturbations. In the LEO region, the dominant perturbation effects are atmospheric drag and J2 geo-potential effect. All the other effects will be neglected in the following analysis, as retained negligible for the level of accuracy sought.

## 4. Ptolemaic filter description

### 4.1. Orbital model and auxiliary representation

The Keplerian orbital model is the one employed today for describing the celestial bodies' motion under the influence of the gravitational pull from a primary body. It describes trajectories through ellipses following the Keplerian laws of motion. The present paper tries to evaluate the possible advantages of employing an orbital description simplification for conjunction analysis, introducing some modelling errors from the Keplerian formulation. This convention can be called *Ptolemaic simplification*, as inspired by the theory of *epicycles* introduced by C. Ptolemy regarding the motion of the planets about Earth. In his model (Heliocentric theory) planets move around Earth in small circles (the epicycles) orbiting in bigger ones (called instead *deferents*). In Figure 3 (on the left) there is the example of Mars orbiting Earth (in one of the two *equants*, the foci computed by Ptolemy to compensate errors in observations) as described by the Ptolemaic theory.

Even if it is clear this model is physically incorrect, it has been recovered here replacing ellipses with off-centric circles. Figure 3 (on the right) represents this auxiliary model: the ellipse is replaced with the off-centric inscribing circle or so-called *deferent*.

It is clear that the deferent model better suits orbits with small eccentricities. The maximum error between the two models can be computed as the distance between the semi-minor and the semi-major axis of the ellipse, or the radius of the different. Table 2 reports some statistics:

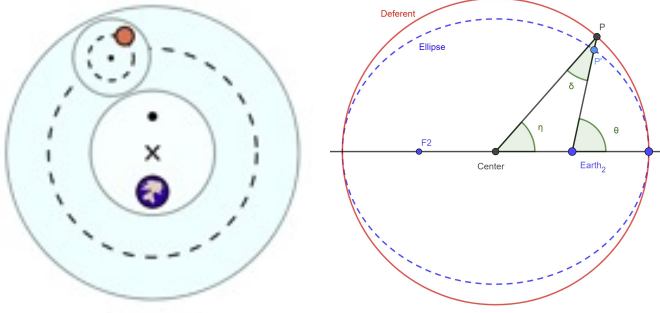


Figure 3: Representation of Ptolemy's theory (on the left) and the actual Ptolemaic model employed in this work (on the right).

Table 2: Ptolemaic model error for orbits in the catalogue.

Maximum error	Number of satellite	Percentage of orbits
< 5 km	7660	98.7%
< 1 km	7600	97.9%
< 0.5 km	7547	97.3%
< 0.1 km	7306	94.1%
< 0.05 km	7010	90.4%

It is clear that for LEO the deferent model is not far from the real one for the great majority of the orbits.

This model will be employed in the next section to set up the filtering technique.

The definition of the deferent requires the four Keplerian parameters:  $a$ ,  $i$ ,  $\Omega$  (right ascension of the ascending node) and  $\omega$  (the argument of perigee), since the eccentricity is neglected. The corresponding time-law can be computed instead on the deferent as the direct projection of the true anomaly in time (like in Figure 3), employing the eccentric anomaly  $E$  instead.

#### 4.2. Ptolemaic filter algorithm structure

The algorithm based on the deferent aims to define if a pair of orbits could result or not close encounters (or conjunctions) over time. It consists of a series of four pre-filters and a final MOID. From now on, all the algorithms presented will consider the deferent model instead of the classic Keplerian one.

Conjunction is defined as an event when two trajectories come closer than a certain threshold distance. In this paper, this threshold is defined as  $D$  (1) (total threshold); this value corresponds to the sum of position uncertainty (due to the Ptolemaic model and perturbed motion) and an effective distance used for comparison. Figure 4 represents this concept: black points stand for the satellite position of two orbits compared on the same plane (the dotted line stands for the plane),  $D_r$  is the effective threshold between orbits and  $D_o$  represents the position uncertainty. The choice of the threshold values chosen for each test of the filter is justified later in the paper (Chapter4.3).

$$D = D_r + 2D_o \quad (1)$$

Figure 5 reports the entire flow of tests composing the filter. Before moving to the filter description, it is important to underline that the tests on a pair of orbits can output two kinds of

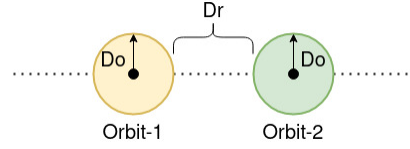


Figure 4: Definition of the threshold for conjunction analysis: black points are single Cartesian points of the trajectories, considered on the same plane and both along-track.

results: no conjunctions or possible conjunctions detected. In case a possible conjunction (red cases in Figure 5) is detected by a test the couple is better inspected and passes to the following one. In case any possible conjunction is stated (green output in Figure 5) the orbit is filtered out, and any further analysis is done.

The original code language of this algorithm is Matlab, but it has been rewritten entirely in Python to better suit more software tools integrations.

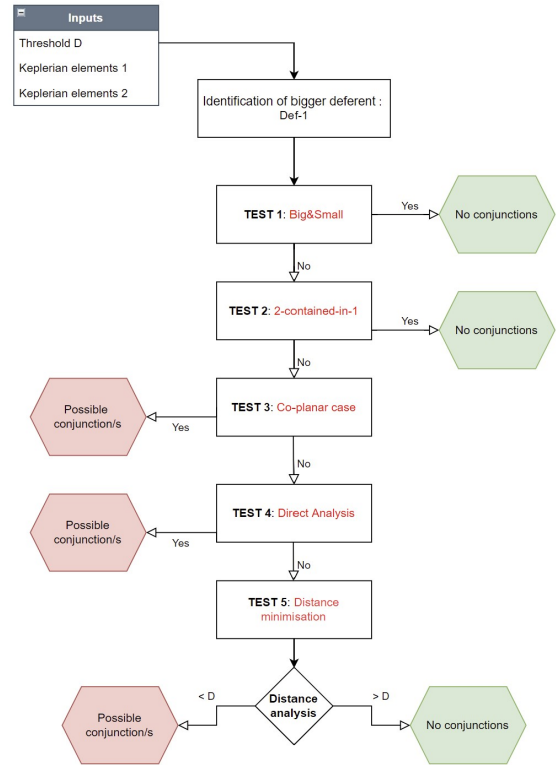


Figure 5: Filter process scheme including the possible outcome for each test.

In the following sections, each test composing the Ptolemaic filter is described.

##### 4.2.1. Description of Test-1: 'Big & Small'

Just before *Test-1* the algorithm classifies as *Def-1* (deferent number 1) the orbit with bigger  $a$  and as *Def-2* the other one<sup>2</sup>.

<sup>2</sup>Subscript 1 and 2 identify the two deferents through all the tests: 1 is the one with bigger  $a$ , as defined in *Test-1*.

Following this notation,  $C_1$  and  $C_2$  will be the centres of the two deferents, and  $c_1$  and  $c_2$  are their effective distances from Earth centre, as reported in Figure 6 (top).

*Test-1* is inspired to the Hoot's *Perigee-Apogee filter*[3]. This test compares the equivalent perigee of *Def-1* (the bigger) and the apogee of *Def-2*:

$$(R_1 - c_1) - (R_2 + c_2) > D \quad (2)$$

where  $R$  is the radius of the deferents and  $c$  the distance of the centres of deferents from Earth centre. In this case, Ptolemy's model simplifies the formulation of the geometry along the algorithm. If the previous equivalence is true any conjunction is possible; otherwise, it is necessary to pass to *Test-2*.

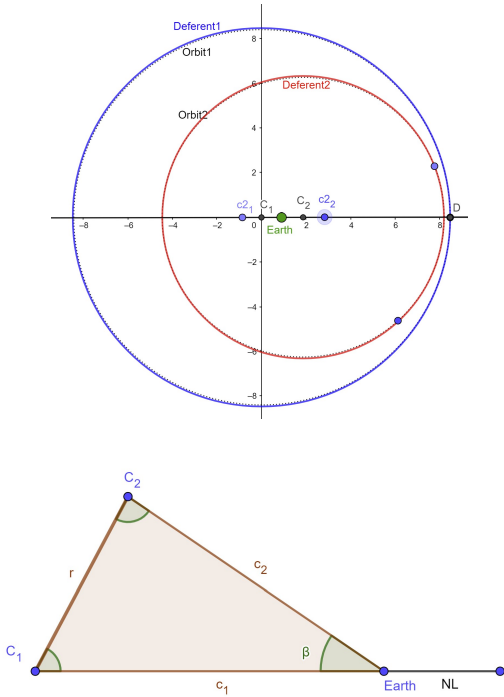


Figure 6: Representation of *Test-1* (top) and *Test-2* (down) geometries.

#### 4.2.2. Description of *Test-2*: '2-contained-in-1'

This test considers the central idea of the Ptolemaic filter: the rotation of one deferent with respect to the other. This transformation could be considered as a simple change of reference frame (RF): the RF that will be used from now on is the perifocal RF of *Def-1*. *Def-2* is rotated from Earth-centred equatorial RF to perifocal reference frame of *Def-1*.

The matrix used for this transformation is the one that converts from equatorial to perifocal the Keplerian orbit, but this time using angles of *Def-1* (formulation of the matrix recalled in Figure 7).

$$Q_{xz} = \begin{bmatrix} \cos(\Omega)\cos(\omega) - \sin(\Omega)\sin(\omega)\cos(i) & \sin(\Omega)\cos(\omega) + \cos(\Omega)\cos(i)\sin(\omega) & \sin(i)\sin(\omega) \\ -\cos(\Omega)\sin(\omega) - \sin(\Omega)\cos(i)\cos(\omega) & -\sin(\Omega)\sin(\omega) + \cos(\Omega)\cos(i)\cos(\omega) & \sin(i)\cos(\omega) \\ \sin(\Omega)\sin(i) & -\cos(\Omega)\sin(i) & \cos(i) \end{bmatrix}$$

Figure 7: Matrix converting from Equatorial to perifocal RFs.

Keplerian angles ( $\Omega$ ,  $\omega$  and  $i$ ) are relative parameters of *Def-2* with respect to *Def-1*. These values are recovered just by rotating the perigee of *Def-2* in perifocal RF of *Def-1*.

Once this step has been performed, *Def-1* will be considered always with its nodal line laying on the  $x$ -axis of the equatorial RF ( $\Omega_1 = 0\text{deg}$ ,  $\omega_1 = 0\text{deg}$  and  $i_1 = 0\text{deg}$ ).

This test wants to verify if the couple of deferents has a configuration such that *Def-2* is 'contained' in *Def-1* (considering also the threshold  $D$ ).

The inequality verifying this condition is the following:

$$R_1 > r + R_2 + D$$

$$r = \sqrt{c_1^2 + c_2^2 - 2c_1c_2\cos(\beta)} \quad (3)$$

$$\beta = \Omega_2 + \omega_2$$

The angle  $\beta$  is the difference between angles  $\Omega$  and  $\omega$  of the two orbits, this is zero for *Def-1*.

Figure 6 shows the geometry used to find the expression. Where the line  $f$  (conjunction between  $C_1$  and Earth) corresponds to the nodal line of *Def-1*.

In case the inequality is satisfied, the couple will never result in possible conjunctions. In all the other cases it is necessary to pass to *Test-3*.

#### 4.2.3. Description of *Test-3*: 'Co-planar-case'

As for many other algorithms found in literature, (e.g. Hoots et al.'s filters [3]), the case of nearly co-planar orbits is a critical case. Even if the relative inclination between orbits is exactly  $i_{rel} = 0\text{deg}$  (co-planar case) is nearly impossible, this borderline case can produce numerical problems or singularities.

In classical tests, the co-planar case is considered when all the points of *Def-2* with respect to the plane of *Def-1* have a vertical distance (out-of-plane) within the threshold  $D$  considered. For the present analysis, a couple will be identified as co-planar, or better *nearly-co-planar*<sup>3</sup>, when the relative inclination (of *Def-2* with respect to *Def-1*) is smaller than  $10^{-3}\text{deg}$ .

This condition has been numerically tested considering some boundary cases too. Let's consider for example:  $a = 180\,000\text{km}$  and  $e = 0.9$ , at a relative  $i$  of  $10^{-3}\text{deg}$ . The apogee will be  $342\,000\text{km}$  and its altitude with respect to *Def-1*'s plane (so the horizontal plane) will be  $5.96\text{km}$ . This can be considered an extreme case (also not in LEO, but good for understanding), producing a very bad Ptolemaic approximation.

If a pair of deferents presents the feature searched for by the test, this couple will certainly produce conjunction somewhere along the orbits, since *Test-2* has failed before.

Other algorithms for co-planar cases have been evaluated before selecting this one. This test however mainly allows us to avoid the case of  $i_{rel}=0$ , which could cause some problems to

<sup>3</sup>Since the perfectly co-planar case is nearly impossible in real orbits.

*Tests-4* and *Test-5*. Furthermore, it is not a particularly time-consuming test, since it just needs to verify the value of the relative inclination.

#### 4.2.4. Description of Test-4: 'Direct Analysis'

Here the configuration of *Test-2* is exploited to shape a test inspecting the two points where deferents cross in perifocal RF of *Def-1*, in other words in the plane of the first orbit.

In practice, there would always be a small relative inclination between orbits (except for the constellation cases), even if small enough, this fact means that there will be always two crossings between *Def-2* and the plane of *Def-1*. Through Ptolemy's approximation, it is easy to identify these points for deferents. These are represented in Figure 8: respectively the white dots in the 3D visualization (top) and L, M blue ones in the planar plot (down).

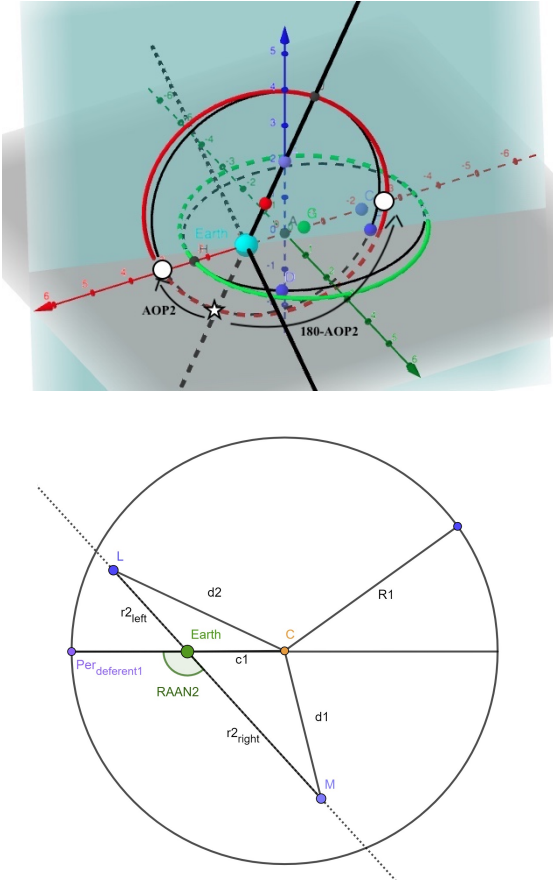


Figure 8: Representation of *Test-4* geometry: in the perifocal RF of *Def-1* (top) and the 3D visualization (down) respectively.

A deeper description of the geometrical procedures leading to this filter setup is provided in Appendix A. If this test detects conjunctions, the couple of deferents does not require more investigations. On the other side, if this test does not detect conjunctions it could be possible anyway that other points around L and M (in *Def-2*) will come closer to *Def-1*. These possibilities are evaluated by *Test-5*.

#### 4.2.5. Description of Test-5: 'Distance-minimization'

This last test inspects possible conjunctions that have not been detected before.

For this last test, it is useful to consider the relative uncertainty  $D$  between deferents as located entirely around *Def-1*, as represented in Figure 9: threshold  $D$  in 3D is a toroid around *Def-1*. In the plot,  $C_1$  and  $C_2$  are the centres of the two deferents, and the blue fill stands for *Def-1* together with the toroidal threshold  $D$  around it. *Def-2* is in black.

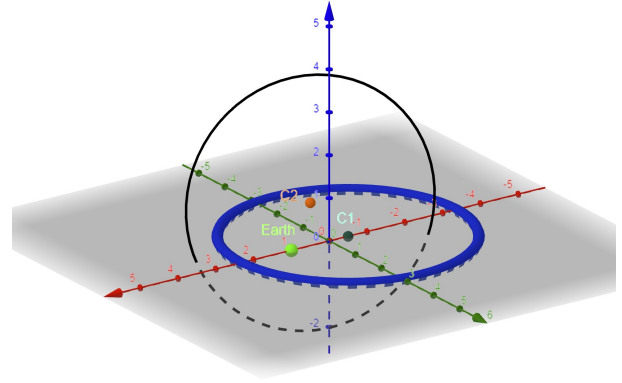


Figure 9: Representation of a random couple of deferents where threshold  $D$  is represented as a toroid around *Def-1* (in perifocal RF of *Def-1*).

This last test goes through a minimum global research routine: it tries to minimise a function corresponding to the relative distance between points on the two deferents, exploiting the advantages of the Ptolemaic model as much as possible.

The deferent model allows a clever formulation of the distance function between the two deferents, the details of this formulation are discussed in Appendix B. This function has just one variable,  $E$  the eccentric anomaly of *Def-2*. The minimisation problem is a bounded problem that can be solved through a Brent-like minimization algorithm. Such an algorithm has been implemented from the works of Forsythe and Brent [15], [16]. It takes as input: the function to be minimized and the bounds for the variable research. The test itself receives in input the orbital parameters of the deferent.

#### 4.3. Perturbations contributions and thresholds deduction

Deferents considered up to now are simply conics derived geometrically from Keplerian parameters, while orbits are perturbed trajectories. In the case of LEO, the most relevant perturbation effects to retain are  $J_2$  geo-potential and drag.

The algorithm explained before is considered to be employed at the level of preliminary filtering of orbits in the conjunction analysis classical pipeline. The present research proposes to add a preliminary propagation of the orbits after the SGP4 propagation, to build up the effective deferent model. This propagation consists of two steps:

- numerical propagation over a 1-day horizon (after SGP4 propagation of 10 seconds) for the entire catalogue

- mean elements filtering for each orbit about the numerical propagation, and averaging the mean elements in time

The numerical propagator has been conceived internally in AIKO, accounting just for J2 geo-potential contribution and drag through an exponential atmosphere model (main references used for the development: [17], [18]). The mean elements filter instead is inspired by the work of Servida [19], based on Ustinov and Kaula's theories ([20], [21]). It includes also an adjustment for the  $a$  estimate, proposed instead by Brouwer and Lyddane [22].

Table 3 reports the performance and accuracy of the numerical propagator, while in Figure 10 the mean elements filtering process is shown for a random orbit of the catalogue.

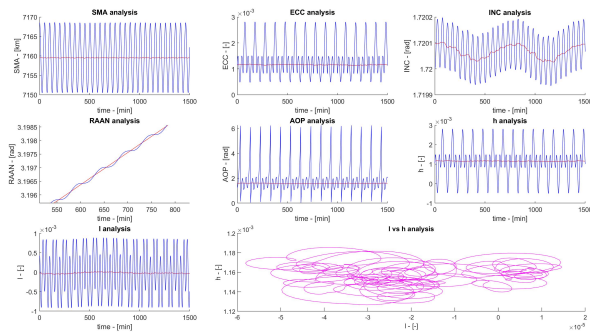


Figure 10: Mean elements (in red) computed with respect to osculating states propagated with the numerical propagator (blue) [1-day propagation].

However, Ptolemy's tests defined before need a single set of elements (Keplerian set) as input. Due to that, mean elements are numerically averaged once computed, in order to derive for each orbit a 'static' set of elements, employed for the geometrical definition of deferents for the filter.

Table 3: Performance of the numerical propagator employed for tests. Accuracy is assessed with respect to propagation computed with the NASA GMAT tool [23].

Tool	1 month	3 months	Accuracy after 1 day
Fast-Num	~ 0.088 s	~ 0.253 s	~ 0.2 km (RMS)

However, defining deferents through a single set of mean elements introduces another error caused by perturbations. In fact, the orbits obtained through mean elements differ from the osculating ones (along one day) in both in-plane (in the plane of the mean elements deferent) and out-of-plane (normally to the deferent plane) distances. The most important contribution is represented by the out-of-plane distance. This fact is very clear in Figure 11. These two plots report for each orbit of the catalogue the distance of any point of the osculating orbit from the mean orbit along the one-day propagation: the in-plane distances (left) and the out-of-plane ones (right).

The insights extracted from this analysis of the catalogues allow to define suitable thresholds employed for the conjunction analysis with the Ptolemaic approach. Since *Test-5* in-

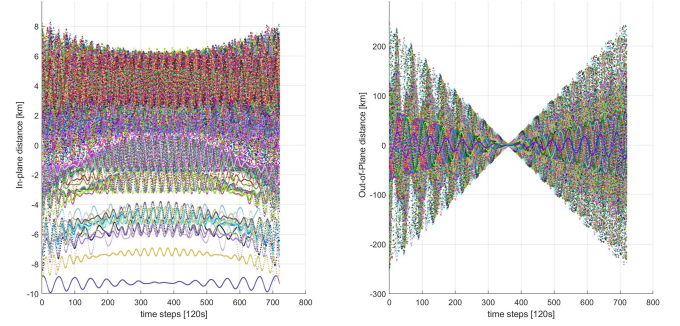


Figure 11: In-plane distance from the mean orbit (left) and out-of-plane distance from the mean orbit (right) for all TLEs.

volves both in-plane and out-of-plane distances, in the deferents comparison, two values of thresholds  $D$  are defined: one for tests involving in-plane distances ( $D_{in}$ , for *Test-1*, *Test-2*, *Test-4* and *Test-5*) and one for tests involving out-of-plane distances ( $D_{out}$ , just for *Test-5*).

Values retained for the present analysis are derived from an inspection of values shown by Figure 11:

- $D_{in-plane} = 25$  km
- $D_{out-of-plane} = 205$  km

The maximum in-plane distance is about 10 km from the mean orbit, while the out-of-plane is 100 km (considering the great majority of the points are under this limit). Thresholds are computed starting from double of the maximum distance adding a five kilometres buffer.

Model accuracy errors due to Ptolemaic approximation are smaller than those of perturbations, and due to that do not impact directly the definition of the thresholds. However, a deep assessment and quantification of the model error introduced have been considered for each test.

It is important to notice that *Test-5* involves both thresholds. Furthermore, this process allows to account for perturbations effects along a certain time period along the filtering analysis, with a minimal computational effort.

## 5. Performance assessment

### 5.1. Benchmark description

The benchmark employed for the performance assessment and validation of Ptolemy's tests is Gronchi's MOID algorithm, well known in the literature as extremely efficient and precise. Gronchi et al. [5] developed an algebraic method allowing to find the sixteen closest geometrical points between the orbits compared, the one which is interesting here, in particular, is the minimum distance (the MOID).

Gronchi's algorithm does not account for any physical model, it relies on a purely geometrical comparison between ellipses. Gronchi's test has been implemented in both Matlab and Python languages for the present work, directly from Gronchi's paper [5]. The algorithm takes as input the Keplerian elements of the two orbits. It returns the minimum distance (MOID) and its

anomaly on the two orbits. In this case, the Keplerian model is considered and the input of the benchmark is the averaged mean elements set of the two orbits.

Ultimately, Gronchi’s algorithm takes approximately  $1e-3$  seconds per couple for MOID computation.

The benchmark employed for the performance assessment of the Ptolemaic filter is a combination of the Gronchi test together with the Hoots’ *Perigee-Apogee* pre-filter (employed before Gronchi). Hoots’ test filters faster orbit couples that would clearly not produce conjunctions that Gronchi’s algorithm alone. This is done in order to make Gronchi’s and Ptolemy’s performance comparable. For these two algorithms, the following thresholds have been considered:

- $D_{Hoots} = 65$  km
- $D_{Gronchi} = 25$  km

Hoots threshold value has been recovered from literature [3]. While the threshold of Gronchi has been set equal to the one of in-plane for Ptolemy’s tests (defined in Chapter 4.3).

## 5.2. Performance evaluation

In this section, both the benchmark and Ptolemaic filter are tested in an all-vs-all analysis. Results are discussed in a comparative analysis with the benchmark approach.

Before propagating the TLEs, it is a good practice to filter them to check errors and inconsistencies in the catalogue: TLEs filters employed here are classical ones (detailed for example in Muciaccia’s work [24]). By applying them, just three TLEs are excluded.

All remaining TLEs are propagated forward with SGP4 to recover osculating positions (in TEME<sup>4</sup> reference frame). After that, all the orbits are propagated with the custom numerical propagator and mean elements are obtained (over a period of 24 hours, time step of 20 seconds). The time spent for this first part (applied to 7 754 orbits) is about 1.86 h, providing propagation results and everything set for the filtering process.

Once mean elements are recovered and averaged, the filtering process is ready to be run. Both Ptolemy and benchmark are tested over the entire catalogue: the total number of orbits is 7754 since 3 have been rejected. This type of analysis is the so-called all-vs-all analysis, considering all couples possible without repetitions (in this case 30 058 381).

Table 4 and table 5 report respectively the results of the conjunction analysis with the Ptolemaic filter series and the one with Hoots + Gronchi. It is important to notice that *Test-1*, *Test-2*, *Test-3* and Hoots’ pre-filter are not capable to classify couples as producing possible conjunctions; while *Test-4* is not enough to state that any possible conjunction is present.

Further analysis of the results highlights the following points:

- the number of conjunctions detected is considerable since many constellations are present in the catalogue (mainly Starlink, COSMOS and OneWebb);
- the Ptolemaic filter detects more conjunctions than the benchmark (around 23% more), which means that it is in general more conservative;
- the Ptolemaic filter is capable to exclude many couples before the final analysis: *Test-1* and *Test-2* exclude more couples than the Hoots’ pre-filter.

Table 4: Results of Ptolemy’s filter run, all-vs-all.

Test	No conj.	Possible conj.	Tot. couples per test
Test-1	20 701 259	-	20 701 259
Test-2	3 202 938	-	3 202 938
Test-3	-	889	889
Test-4	-	1 515 781	1 515 781
Test-5	4 079 623	557 891	4 637 514
Tot		2 074 561	30 058 381

Table 5: Results of Gronchi + Hoots’ filter run, all-vs-all.

Test	No conj.	Possible conj.	Tot. couples per test
Hoots	17 769 948	-	17 769 948
Gronchi	10 583 179	1 705 254	12 288 433
Tot		1 705 254	30 058 381

A deeper analysis has been conducted about the couples classified as conjunctions through the Ptolemaic approach: this subset includes all the couples detected by Gronchi’s MOID as a conjunction. This is a very important result, as it validates the Ptolemaic approach itself. The gap in conjunctions detected between the two approaches is mainly due to *Test-5*, which employs a huge threshold for out-of-plane distances.

Table 6 instead presents the CPU times spent by the two algorithms for the entire all-vs-all analysis, except for the algorithms initialization (times are computed as an average of three consecutive runs).

Table 6: CPU time estimate for each approach.

Algorithm	Tot. CPU time
Ptolemy	3 656.0 ± 1.5 sec ( $\approx$ 1.0 h)
Hoots+Gronchi	13 323.0 ± 1.5 sec ( $\approx$ 3.7 h)

In this configuration, the Ptolemaic algorithm is faster than the benchmark considered. However, this comparison could be done also adding further pre-filters before Gronchi’s algorithm in order to further improve performance. These results prove the efficiency of the test pipeline in the Ptolemaic filter.

An average of the times taken by the single tests is reported here (along with the all-vs-all analysis):

- Test-1:  $6.5 \cdot 10^{-5}$  s /couple
- Test-2:  $7.9 \cdot 10^{-5}$  s /couple
- Test-3:  $5.3 \cdot 10^{-5}$  s /couple
- Test-4:  $5.9 \cdot 10^{-4}$  s /couple

<sup>4</sup>True Equator Mean Equinox, the reference frame of TLEs used in SGP4

- Test-5:  $9.5 \cdot 10^{-4}$ s /couple

It is important to notice that also *Test-5* is faster or at least comparable to Gronchi’s algorithm.

## 6. Derived AI-based pipeline including the Ptolemaic approach

Once seen the advantages such an approach can introduce in the very first part of the conjunction pipeline, it has been hypothesised its inclusion inside an AI-based pipeline. As already evaluated in some previous researches (e.g. Stevenson and Rodriguez [10]) considering an AI-based algorithm inside the conjunction analysis process could contribute in increasing the efficiency in the research of conjunctions or the filtering of couples. In this paper it has been considered for the pipeline a machine learning algorithm (ML). The task of conjunction detection can be considered a binary classification task for a ML-algorithm, in which the model learns to predict a class label starting from a training set of observations for which the true class is already known. The dataset of the learning process in this case is the amount of couples to compare (specifically the orbital sets of Keplerian elements).

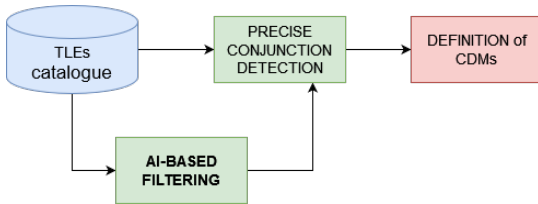


Figure 12: Conjunction analysis pipeline introducing possible AI-based pre-filtering.

One of the main hurdles along the AI algorithm implementation inside the conjunction analysis is the unbalance of the dataset considered: the amount of effective close conjunctions is much smaller than the total amount of couples considered. The possible improvement introduced by considering the Ptolemaic model inside the AI-pipeline is related to the training phase. As described before in fact the Ptolemaic approach allows to condense in the model itself the perturbation contributions in the formulation. The block of AI filtering could be employed as a pre-filtering phase, allowing to exclude a certain amount of couples not producing conjunctions, and leaving the final and more precise analysis to classical approaches.

## 7. Conclusions and next steps

### 7.1. Main conclusions

The present work has validated the potential behind an approximated orbit model employed for conjunction detection. The Ptolemaic filter, which employs a deferent model, has been proven to be efficient and reliable as compared with well-known benchmarks (Hoots and Gronchi). Another advantage is the fact that the algorithm is built through the study of the orbital

parameters’ evolution in time, containing propagation information. Indeed, it allows to take into account a better evolution of the orbit through the definition of the thresholds starting from mean elements. Despite these additional capabilities, this feature does not add considerable computational time.

Furthermore, *Test-1* and *Test-2* together are capable to exclude a good amount of couples (around 24 million), making the entire process very efficient. In particular, the first two tests of the Ptolemaic filter exclude about 27% more couples than the Hoots’ pre-filter.

In conclusion, the main advantage that the algorithm provides is the capability to efficiently filter out a great number of couples. This has been obtained thanks to the many simplifications introduced by the deferent model in the geometrical formulation, considering a circle instead of an ellipse. Still, it is important to keep in mind that the Ptolemaic model introduces two errors: a modelling error and an error due to the mean elements-based geometry.

The present algorithm shows potential for being used in the very first phase of the conjunction analysis, where the filtering of the couples is performed. Furthermore, the possibility to better include propagation information in the filtering process could improve it in some ways: keeping the information about the perturbation maximum oscillations around mean elements, can be used for better estimates of future possible conjunctions.

### 7.2. Possible next steps

The present research tries to inspect the possible advantages of an alternative conjunction analysis approach, improving computational performance and allowing for a thorough consideration of perturbation effects.

Some improvements have been already identified as the next efforts for the present research.

The first potential improvement for the algorithm is MOID detection. The actual algorithm does not consider time phasing between objects (or their hour-angle). The first step towards that would be to include anomaly inspection in the conjunction detection (e.g. for conjunction detected by *Test-5*).

The second potential improvement is the inspection of a longer mean elements evaluation: evaluating the orbit mean elements filtering for a wider time span and its consequences.

Another improvement concerns the integration of this algorithm in an AI-based pipeline. Modern conjunction detection pipelines consider introducing also AI-based algorithms in order to improve the conjunction detection process efficiency. In particular, the present model could be employed in the training phase of the AI algorithm; allowing to make a longer and more reliable prediction of orbit evolution and conjunction estimate.

## Appendix A. - Test-4 description

*Test-4* setup is better described here.

The following steps allow computing the two crossing points required for *Test-4*, between the *Def-2* and *Def-1*'s plane.

1. Since *Def-2* has been translated in perifocal RF of *Def-1*, the two points we are looking for belong exactly to the nodal line of *Def-2*. Moreover  $\Omega_2$  is simply the angle from the perigee of *Def-1* up to the line of crossing between the planes of orbits. Crossing points are represented in Figure 8 (down): L and M. Where C is the centre of *Def-1*.

2. Exploiting previous deductions, two useful triangles could be identified (Figure 8) on the plane of *Def-1*: the first one for the point M ( $Earth - \hat{C} - M$ ), and the second for point L ( $Earth - C - L$ ).

What is needed to set up *Test-4* are distances  $d1$  and  $d2$  (represented in Figure 8), from the centre of *Def-1*. Once obtained, it will be straightforward to compare these distances with  $R_1$ , to verify conjunctions at these two locations.

3. In order to obtain  $d1$  and  $d2$ , the two previous triangles are solved. Since it is already known the common side  $c_1$  (the ellipse parameter of *Def-1*), at least another side and one angle are needed.

Angles between  $c_1$  and the two sides  $r_{2,ight}$  and  $r_{2,left}$  (distances of L and M from Earth) could be easily computed with  $\Omega$  of *Def-2*, assuming point (1).

$$\begin{aligned} (C - Earth - M) &= 180 \text{ deg} - \Omega_2 \\ (C - Earth - L) &= \Omega_2 \end{aligned} \quad (A.1)$$

4. Distances from Earth of points L and M are computed instead considering the geometrical definition of  $\omega$  for *Def-2*. The procedure is the one represented in Figure 8b. In this representation *Def-1* is the green one, while *Def-2* is the red one; L and M are the two big white points. The two distances are computed by recovering eccentric anomalies from true anomalies (the one represented in Figure 8).

5. Through a well-known theorem, knowing two sides of a triangle and the angle between them the geometry can be solved. In one step more  $d1$  and  $d2$  are computed.

Once distances  $d1$  and  $d2$  are computed, the aim of this test is to verify if these two points come closer than  $D$  to *Def-1*. This could be verified through the following inequalities:

$$\begin{aligned} |R_1 - d_1| &> D \\ |R_2 - d_2| &> D \end{aligned} \quad (A.2)$$

In case inequalities are both verified any conjunction is possible at these two points; from the sign of the two differences we can understand if L and M stay inside or outside *Def-1*.

## Appendix B. - Test-5 description

In this appendix a more in-depth description of *Test-5* is provided.

Since *Def-1* lays completely on the horizontal x-y-plane of the main RF (due to the rotation performed, in its perifocal RF), the relative distance between deferents can be computed as the sum of the squares between distance from  $C_1$  (planar distance) and elevation (out-of-plane distance) from the *Def-1* plane, for all points on *Def-2*. Once the minimum distance is found, it is possible to state if any conjunction will happen or not: if the minimum distance is bigger than  $D$  no conjunctions are possible, otherwise at least one is present.

The relative distance between deferents is reshaped as a function of the eccentric anomaly  $E$  of *Def-2* ( $E_2$ ): this is called  $F$ , the function to be minimized. This is defined here:

$$\begin{aligned} F &= f(E_2) \\ F &= \sqrt{(|\vec{P}_{Def-2} - \vec{C}_1| - a_1)^2 + z_p^2} \end{aligned} \quad (B.1)$$

where  $\vec{P}$  is the position vector of a generic point on *Def-2* and  $z_p$  is its elevation from horizontal plane (*Def-1*'s plane). And  $\vec{C}_1$  is the position vector of the *Def-1* centre. The  $F$  function is simply the planar distance from *Def-1* together with the vertical distance from the plane of *Def-1*. Adding the two contributions, the resulting distance constitutes the relative distance between deferents.

The passages to obtain  $F$  are reported in the following equation:

$$\vec{P}_{perifocal2}(E_2) = \begin{bmatrix} (a_2 \cos(E_2) - a_2 e_2) \\ (a_2 \sin(E_2)) \\ 0 \end{bmatrix}$$

$$\vec{P}_{perifocal1} = \bar{Q}_{xx} \vec{P}_{perifocal2}$$

$$z_p(E_2) = \vec{P}_{perifocal1}(3)$$

$$F(E_2) = \sqrt{(\sqrt{(\vec{P}_{perifocal1}(1) + c_1)^2 + \vec{P}_{perifocal1}(2)^2} - a_1)^2 + z_p^2} \quad (B.2)$$

$\bar{Q}_{xx}$  is the matrix providing transformation from perifocal to equatorial RF with angles of *Def-2* relative to *Def-1*, this matrix is not a function of  $E$ .  $\vec{P}_{perifocal1}$  is the position vector on *Def-2* in perifocal frame of *Def-1* at the anomaly selected. The function  $F$  provides the relative distance between the two deferents. Once minimised this function, it is sufficient to compare its minimum with the threshold  $D$  and verify if at least one conjunction is present or not.

This function is minimised through the algorithm described before. The characteristics of this function are the following:

- single variable function;
- non-linear function;
- $F$  presents probably more than one local minima.

Along the conjunction analysis, in *Test-5* both in-plane and out-of-plane thresholds are involved. The minimum found is firstly checked for the out-of-plane distance and in case it is smaller, it is checked for the in-plane too.

## Acknowledgements

I want to thank my colleague Paolo Madonia (AIKO) for the support and review of the paper, together with Alessandro Benetton and Davide Vittori (AIKO) who have trusted me in carrying on this research internally.

## References

- [1] T. Share My Space SAS, Space sustainability bulletin (Dec. 2022).
- [2] G. Sirtarski, Approaches of the parabolic comets to the outer planets, *ACTA Astronomica* 18 (2) (1968).
- [3] F. Hoots, R. Roehrich, Models for propagation of norad element sets, Defense Documentation Center (Alexandria) (1988).
- [4] K. Kholshchikov, Close encounters, *Celestial Mechanics and Dynamics Astronomy* 91 (278) (2005).
- [5] G. F. Gronchi, An algebraic method to compute the critical points of the distance function between two keplerian orbits., *Celestial Mechanics and Dynamics Astronomy* 93 (295-329) (aug 2005).
- [6] C. Bonanno, An analytical approximation for the moiré and its consequences, *Astronomy and Astrophysics* 306 (411) (2000).
- [7] A. Lidtke, D. Gondelach, R. Armellin, Optimising filtering of two-line element sets to increase re-entry prediction accuracy for gto objects, *Advances in Space Research* 63 (2019) 1289–1371.
- [8] Z. Knezevic, A. Milani, Synthetic proper elements for outer main asteroid belt, *Astronomical observatory* 78 (17) (2001).
- [9] A. Rozek, S. Breiter, T. Jopek, Orbital similarity functions – application to asteroid pairs, *Monthly Notices of the Royal Astronomical Society* 412 (sep 2010).
- [10] U. H. Stivenson E, Rodriguez V., Artificial intelligence for all vs. all conjunction analysis, 8th European Conference on Space Debris (2021).
- [11] F. Hoots, L. Crawford, R. L. Roehrich, An analytic method to determine future close approach between satellites, *Celestial Mechanics* 33 (143-158) (1984).
- [12] D. Vallado, P. Cefola, Two-line element sets - practice and use, *International Astronautical Congress* (2012).
- [13] U. S. F. NORAD, Spacetrack, last access on: Jan 10, 2023.  
URL <https://www.space-track.org>
- [14] T. Kelso, Frequently asked questions: Two-Line Element set Format, 1st Edition, CELESTRACK website, 2004, ( See: <https://celestrak.com/columns/v04n05/> ), last access on: January 10, 2023.
- [15] M. A. M. Forsythe, G.E., C. B. Moler, Prentice-hall series in automatic computation, *Computer Methods for Mathematical Computations* 78 (17) (1977).
- [16] R. P. Brent, Algorithms for minimization without derivatives, Courier Corporation (2013).
- [17] Toronto-University, Hypernova (2007).  
URL <https://github.com/utat-ss/hypernova>
- [18] M. Mahooti, High Precision Orbit Propagator, MATLAB Central File Exchange, <https://www.mathworks.com/matlabcentral/fileexchange/55167-high-precision-orbit-propagator> (apr 2021).
- [19] P. Servidia, M. Espana, Fast and reliable computation of mean orbital elements for autonomous orbit control, *Unidad de Formacion Superior* (nov 2019).
- [20] W. Kaula, Theory of Satellites Geodesy, 1st Edition, Waltham MA: Blaisdell Publishing Co., 1966.
- [21] B. Ustinov, Motion of satellites along low-eccentricity orbits in a non-central terrestrial gravitational field, *Cosmic research* 5 (1967).
- [22] R. Lyddane, Small eccentricities or inclinations in the brouwer theory of the artificial satellite, *The Astronomical Journal* 68 (8) (1963) 555–558.
- [23] NASA, Gmat, last access on: Jan 10, 2023.  
URL <https://sourceforge.net/projects/gmat/>
- [24] A. Muciaccia, Fragmentation in low earth orbit: event detection and parent body identification, Master thesis, Politecnico di Milano. Faculty of Industrial and Information Engineering, DAER, Master in Space Engineering. Supervisor: Camilla Colombo, Co-Supervisor: Matteo Romano (2019).